Streamlined etch integration with a unique neutral layer for self-assembled block copolymers (BCPs)

Mary Ann Hockey, Kui Xu, Yubao Wang, Douglas J. Guerrero, and Eric Calderas
Brewer Science, Inc., 2401 Brewer Drive, Rolla, MO, USA 65401

ABSTRACT

A multifunctional hardmask neutral layer (HM NL) was developed to improve etch resistance capabilities, enhance reflectance control, and match the surface energy properties required for polystyrene block copolymers (PS-*b*-PMMA). This HM NL minimizes the number of substrate deposition steps required in graphoepitaxy directed self-assembly (DSA) process flows. A separate brush layer is replaced by incorporating neutral layer properties into the hardmask to achieve microphase separation of BCP during thermal annealing. The reflection control and etch resistance capabilities are inherent in the chemical composition, thus eliminating the need for separate thin film layers to address absorbance and etch criteria. We initially demonstrated successful implementation of the HM NL using conventional PS-*b*-PMMA. A series of BCP formulations were synthesized with L_0 values ranging from 28 nm to 17 nm to test the versatility of the HM NL. Quality "fingerprint" patterns or microphase separation using 230˚-250˚C annealing for 3-5 minutes was achieved for an array of modified BCP materials. The HM NL had water contact angles at 78˚-80˚ and polarities in the 5-6 dyne/cm range. The scope of BCP platform compositions evaluated consists of a 20˚ water contact angle variance and a 10-dyne/cm range in polarities. All BCP derivatives were coated directly onto the HM NL followed by thermal annealing followed by SEM analysis for effective "fingerprint" patterns. We offer a simplified alternative path for high etch resistance in a graphoepitaxy DSA flow employing a single-layer hardmask for etch resistance demonstrated to be compatible with diverse BCP-modified chemical formulations.

Key Words: Directed Self-Assembly (DSA), Block Copolymers (BCPs), Hardmask Neutral Layer (HM NL)

1. INTRODUCTION

The increasing demand for smaller microfabricated devices requires a continuous shrink in the feature size of device components. Conventional photolithography techniques become incrementally difficult and costly as the feature size requirement approaches less than 20 nm. An alternative approach to generate nanoscale patterns is the directed self-assembly (DSA) of block copolymers (BCPs), which can feasibly provide highly ordered patternable morphologies such as lamellae or cylinders at molecular level size (<20 nm). Polystyrene-block-poly(methyl methacrylate) (PS-*b*-PMMA) has been the benchmark BCP platform material for BCP DSA lithography research and development, but the minimum feature size that PS-*b*-PMMA can achieve is limited to ~ 11 nm because of its low interaction parameter (χ, a fundamental measure of the block incompatibility in the BCPs).[1] High-χ BCPs, which usually contain highly polar blocks, fluorine-rich blocks, or silicon-rich blocks (e.g., polystyrene-block-2-vinylpyridines (PS-*b*-P2VP),[2] polystyrene-block-polydimethylsiloxane (PS-*b*-PDMS),[3] polystyrene-block-poly(2,2,2-trifluoroethyl methacrylate) (PS-*b*-PTFEMA),[4] etc.), are thus under intense research for obtaining 10-nm and sub–10 nm patterns. However, high-χ BCPs are generally difficult to direct and orientate their DSA morphologies due to the disparate polarities and properties between blocks.

Specifically, perpendicular orientation of thin film BCP-DSA is desired for lithographical applications to generate useful nanoscale patterns on substrates, particularly for lamellae-forming BCPs. Most known high-χ BCPs cannot easily form perpendicularly orientated morphology by simple thermal annealing as can be accomplished using PS-*b*-PMMA. They need either an extra top-coat layer or solvent annealing to obtain perpendicular orientation, which can greatly increase the manufacturing cost and complication.[5,6] A key driving force for the Brewer Science neutral layer development was to simplify process flow steps and develop a single neutral layer spin-on coating and to develop multiple types of BCP platforms that were able to form lamellae using high-χ BCPs without the need for a top coat or for complex solvent annealing conditions. The simplified process flow sequence is shown in **Figure 1.**

Alternative Lithographic Technologies VI, edited by Douglas J. Resnick, Christopher Bencher, Proc. of SPIE
Vol. 9049, 90492A · © 2014 SPIE · CCC code: 0277-786X/14/$18 · doi: 10.1117/12.2046351
M.A. Hockey, K. Xu, Y. Wang, D.J. Guerrero, E. Calderas, "Streamlined etch integration with a unique neutral layer for self-assembled block copolymers (BCPs)," Proceedings of SPIE, vol. 9049, paper no. 90492A, 2014.

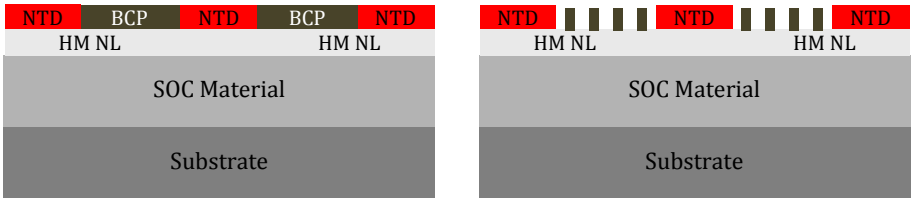

a) Before thermal annealing b) After thermal annealing

Figure 1. Process flow for BCP lamellae using a hardmask neutral layer (HM NL).
NTD = negative-tone development.

2. EXPERIMENTATION

2.1 Materials and Initial Screening Tests Utilized

Current process flows incorporate a wide range of commercially available BCP materials with varying molecular weight targets. We developed customized BCP platforms by combining new types of monomers into the polystyrene block of PS-*b*-PMMA. This work required systematic changes to the PS block in order to achieve a range of surface energy conditions. In addition to the surface energy variations studied, the polystyrene modifications included enhanced etch resistance properties. The goal was to investigate formulations that have the potential to improve the etch selectivity of the PMMA to PS during dry-etch pattern transfer. Typical values for the selectivity of PS-*b*-PMMA are in the range of 2:1 (PMMA:PS). We generated BCP materials that are capable of PMMA:PS etch selectivity of >4:1.

Each BCP material underwent a series of screening analytical tests upon completion of the synthesis process. Initial platforms were measured for molecular weight and polydispersity using gel permeation chromatography (GPC). Examples of several BCP results are shown in **Table I.** The goal was to achieve as low a molecular weight as feasible and polydispersity in the range of 1.15-1.25 for BCP test samples.

Table I. Molecular weight and polydispersity (normalized by standard deviation).

Material ID	Mw normalized	PDI normalized
Material 1	0.64	-0.58
Material 2	0.25	0.25
Material 3	-0.34	0.63
Material 4	0.08	0.04
Material 5	-0.63	-0.38

Validation for the robustness of the enhanced BCP film was quantified using a thickness loss test performed on a Brewer Science® Cee®100 coat and bake stand-alone tool. Spin-coating speeds varied from 1000 to 2000 rpm in 250-rpm increments. The ramp rate was 10,000 rpm/s with a duration of 60 seconds. A two-stage bake was performed at 180°C for 3 minutes, followed by 240°C for 2 minutes. Initial thickness was measured on the M2000 VUV-VASE tool, which was followed by applying a 60-second puddle of PGMEA onto the coated and baked films and spinning dry at 1000 rpm for 30 seconds. A second thickness measurement on the M2000 VUV-VASE tool was performed to determine the thickness loss. Percentage of thickness loss was one quantitative metric that determined the selection of materials utilized for further processing. Note: The initial bake at 180°C was designed to anneal the material, and the subsequent 240ºC bake was required for crosslinking the BCP with monomers added. All materials selected for continued evaluations measured less than 2% for thickness loss. Good compatibility of BCP with the HM NL and pre-patterned photoresist guide structures was validated targeting thickness loss as one criterion. Values measured at >2% thickness loss consistently resulted in poor thermal anneal upon SEM analysis (specifically, “intermittent” or no fingerprint patterns).

The chemical formulations' optical refractive index and absorbance values (n & k) obtained using the M2000 VUV-VASE are shown in **Table II**. Typical k-values range from 0.39 to 0.53 for the BCP materials evaluated.

Table II. BCP optical properties measured at 193-nm wavelength.

Material ID	Thickness (nm)	n-value (193 nm)	k-value (193 nm)
Material 1	30	1.54	0.53
Material 2	30	1.58	0.47
Material 3	30	1.65	0.42
Material 4	29	1.62	0.39
Material 5	29	1.61	0.43

The HM NL was coated onto blank silicon substrate wafers with a thickness target ranging from 25 nm to 30 nm and was baked at 240°C for 1 minute. Each BCP studied then was coated directly onto the hardmask followed and then underwent a two-stage annealing process (180°C for 3 minutes and 240°C for 2 minutes). "Fingerprint" patterns (representative of successful microphase separation) were analyzed using the JEOL SEM **(Figure 2)**. Measurements to determine the L_0 of each material were accomplished using Image J software. Six locations per SEM image were averaged for L_0 values obtained. At each of the locations, five to ten lines and spaces were measured to determine average pitch values **(Figure 2 and Table III).**

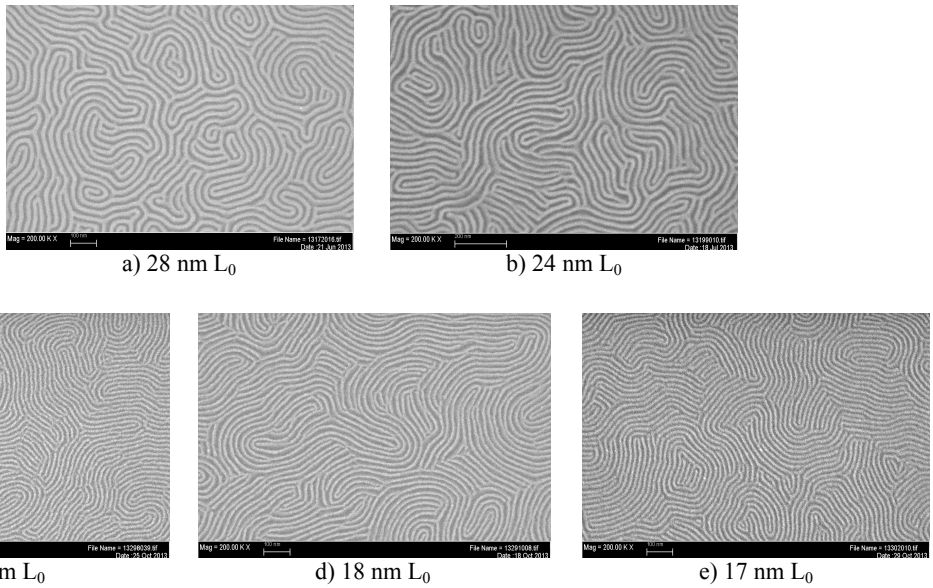

a) 28 nm L_0 b) 24 nm L_0

c) 20 nm L_0 d) 18 nm L_0 e) 17 nm L_0

Figure 2. BCP fingerprints for L_0 materials ranges a) 28 nm, b) 24 nm, c) 20 nm, d) 8 nm, and e) 17 nm.

Table III. Measured L_0 at multiple locations per SEM image using *ImageJ* software.

Material ID	L_0 Value (nm)	Lines/Spaces (nm)
Material 1	28.0	14.0
Material 2	24.0	12.0
Material 3	20.0	10.0
Material 4	18.0	9.0
Material 5	17.0	8.5

2.2 Graphoepitaxy Lithography Testing Strategy

After successful microphase separation was confirmed and measured, the materials were then coated onto wafers pre-patterned with guide structures developed into photoresist by means of 193-nm NTD. The process flow for the pre-patterned wafers included first applying the HM NL on top of a 100-nm spin-on carbon (SOC) layer. Application of all SOC, HM NL, and BCP materials and the resist hard bake were done on a TEL CLEAN TRACK ACT12 under N_2 atmosphere. Substrate layers forming the directed self-assembly patterning were baked at 240°C for 1 minute. The BCP anneal consisted of a two-stage bake at 180°C for 3 minutes and 240°C for 2 minutes; the second stage was used to crosslink the BCP. Just prior to coating the BCP, the photoresist was hard baked at 200°C for 5 minutes. Lines and spaces creating the guide structure were formed on an ASML XT 1250D scanner using negative-tone photoresist (from FUJIFILM Electronic Materials), 0.85 NA using dipole illumination with an outer sigma of 0.93 and inner sigma of 0.69. **Figure 3** shows examples of the results achieved using the NTD guide structures for BCP alignment. The quality and overall dimension size of the guide structures was critical for successful alignment inside photoresist pre-patterns.

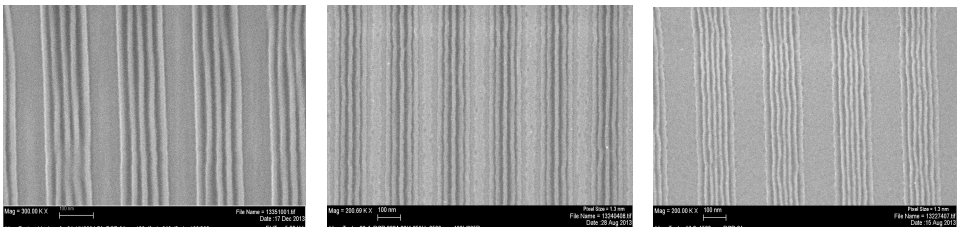

Figure 3. Alignment of BCP materials with 193-nm NTD spaces (100 space/225 pitch).

2.3 Etch Characterization and Pattern Transfer Methodology

An Oxford PlasmaLab80+ etch tool was utilized for etch patterning work. Bulk etch rates on blanket substrates were measured to determine etch values using homopolymer blends of polystyrene. Our experiments included multiple monomers added to the polystyrene at varying concentration percentages targeted to further enhance etch resistance in O_2 plasma. Hompolymer testing of each monomer took place prior to synthesizing the BCP for testing. Results in **Figure 4** summarize typical homopolymer etch rates using a range of etch recipe parameters. These data consistently showed that the standard polystyrene etch rate relative to PMMA can be adjusted to increase selectivity to 4:1 or 6:1 from 2:1 depending on the plasma etch recipe selection and the modified polystyrene type evaluated.

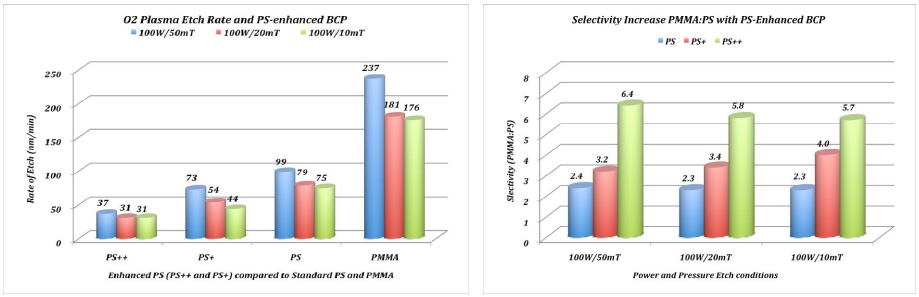

(a) Etch rates in of polystyrene (PS) in O_2 (b) Selectivity of PMMA:PS

Figure 4. (a) Homopolymer etch rates for enhanced PS and PMMA and (b) corresponding selectivity of PMMA:PS.

The annealed BCP etch process included multiple-stage etch pattern transfer steps. The first step was the BCP faster etching block (PMMA) removal step followed by the HM NL etch process. Etch rate characterization of the hard mask neutral layer using a range of power, pressure, and flow conditions is summarized in **Figure 5**.

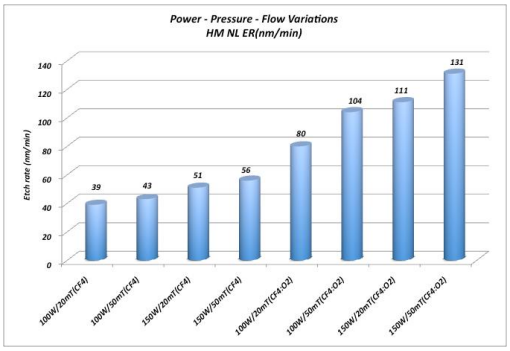

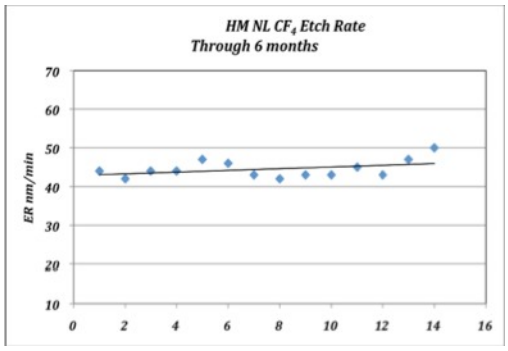

Figure 5. Oxford PlasmaLab 80+ etch rates for HM NL. Figure 6. Consistency of HM NL etch rate for 6 months.

Validation of the material stability for etch quality over time was also studied for a 6-month duration to determine long-term chemical stability, as shown in **Figure 6**. The 45-nm/min etch rate in CF_4 gas was shown to be stable with a standard deviation of less than 5 nm/min. In addition to the etch rate stability, BCP "fingerprint" images were compared for successful microphase separation initially performed on Day 2 and duplicated using the same material after 6 months to determine the HM NL robustness. The results are shown in **Figure 7**.

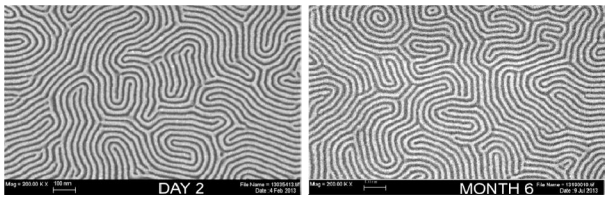

Figure 7. BCP Material 2 and HM NL "fingerprints" from Day 2 (left) through Month 6 (right).

Results of the HM NL etch pattern transfer to date using Materials 2 and 3 are shown in **Figures 8 and 9**. Both argon + O_2 and O_2 only were utilized successfully for etching the PMMA block of the BCP, leaving behind 70-80% of the modified polystyrene for etch protection during the etch transfer through the HM.

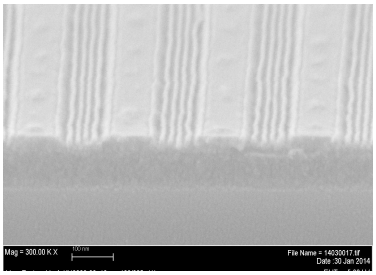

Figure 8. 75° tilt SEM of BCP Material 3 and HM NL in 193-nm NTD pre-patterns.

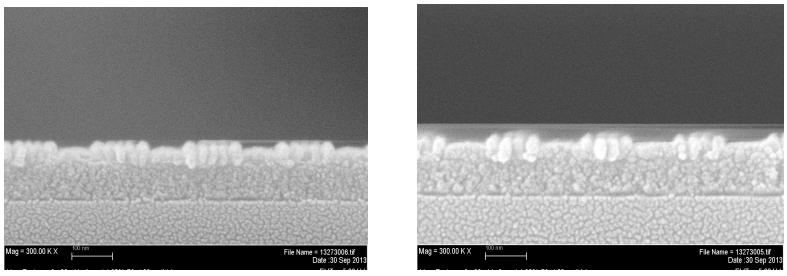

Figure 9. Cross-section SEM of BCP Material 2 and HM NL in aligned pre-patterns.

3. RESULTS AND DISCUSSION

3.1 Surface Energy Effects

Information on the contact angle using water and methylene iodide droplets to calculate polar, dispersive, and total contact angle was gathered for the BCP materials synthesized. The surface energy measurements were obtained using a goniometer. The shape of static liquid droplets dispensed onto the surface of the coated HM NL was measured. The slope of the tangent at the liquid-solid-vapor (LSV) interface and the liquid droplet shape were used to determine the contact angle and calculate surface energy values. Three measurements per substrate were averaged for each contact angle test. A comprehensive study for this characteristic indicates that there is a correlation of total surface energy for the BCP that corresponds to the quality thermal annealing and good fingerprint patterns. Data in **Table IV** summarize the measurements for various formulations of BCP to quantify their surface energy values.

Table IV. Values for BCP surface energy (dyn/cm) with corresponding contact angles.

Material BCP ID	Thickness (nm)	H_2O Contact Angle (°)	Polar (dyn/cm)	Total (dyn/cm)	Fingerprints
50	30	68	10.2	43.6	Yes
05	30	66	12.0	43.4	Yes
60	40	68	11.2	42.9	Yes
10	30	68	10.6	42.7	Yes
20	30	72	8.2	42.4	Yes
30	30	72	7.7	41.6	Yes
25	35	77	5.0	41.5	Yes
40	35	75	7.0	40.9	Yes
21	30	79	4.7	40.7	Yes
31	25	80	4.4	39.5	No
26	25	81	3.9	39.3	No
36	25	82	3.5	39.2	No

As total surface energy approaches values below 40 dyn/cm, the quality of thermal annealing no longer provides consistent fingerprint images. (Water contact angles also begin to exceed 80°). The polar energy of the HM measures in the 5-6 dyn/cm range, and as the BCP materials exhibit values lower than the HM, intermittently poor microphase separation is seen after thermal annealing. The HM NL requires additional modifications to accommodate low values of BCP surface energy (below 40 dyn/cm), high water contact angle materials (>80˚C), and polar energy lower than 5-6 dyn/cm.

4. PROCESS IMPLEMENTATION

Data indicate that the HM NL offers one spin-on coating step that significantly streamlines the process flow for DSA. Current work underway at IMEC for this application is the use of the Brewer Science HM NL for contact level "shrink" processing with the end goal of achieving electrical via chain resistance data. (See SPIE Publication 9049-56, "Evaluation of integration for contact hole graphoepitaxy DSA: A study of substrate and template affinity control," A. Romo-Negreira, Toyko Electron Europe Ltd., et al.) In addition to this process implementation work at contact and via levels, we have further investigated the versatility of our HM NL in this study with a range of BCP materials targeted for line and space multiplication schemes. The goal was to determine the HM NL versatility using multiple types of enhanced BCP formulations with varying surface energy properties.

5. CONCLUSIONS

The ability to utilize a HM NL offers these characteristics and process advantages:

1. Replaces the "brush layer" – PS-r-PMMA – and enables BCP DSA with HM only.
2. Enhances etch resistance for pattern transfer over standard brush layers.
3. Incorporates inherent absorbance (k-value of 0.4-0.5 for 193-nm wavelength).
4. Is a crosslinked system for resistance to solvents (n-butyl acetate) with alignment in NTD pre-patterns.
5. Is capable of both horizontal and vertical (perpendicular – cylinders) DSA.
6. Transfers pattern (l/s) with SOC as an underlayer in a trilayer scheme.
7. PS-*b*-PMMA demonstrated line multiplication line/space features using a guide layer.
8. Contact hole application successful by shrinking 80-nm size to ~25-nm features using graphoepitaxy.
9. Wide surface energy range of BCPs successfully microphase separated using thermal annealing.
10. Thin coatings (25-30 nm) capable of good etch resistance.
11. Compatible with a wide range of commercially available BCP materials.

6. REFERENCES

[1] Nealey, P. F., Bates, F. S., Kim, S., "Block copolymer materials for directed assembly of thin films," U.S. Patent Application No. US 20130029113.

[2] Cheng, J., Lai, K., Li, W., Na, Y. H., Rettner, C., Sanders, D. P., "Directed self-assembly of block copolymers using segmented prepatterns," U.S. Patent No. US8398868.

[3] Millward, D. B., "Methods using block copolymer self-assembly for sub-lithographic patterning," U.S. Patent No. US7964107.

[4] Ellison, C. J., Cushen, J., Otsuka, I., Wilson, C. G., Bates, C. M., Easley, J. A., Borsali, R., Fort, S., Halila, S., "Oligosaccharide/silicon-containing block copolymers for lithography applications," U.S. Patent Application No. US20130022785.

[5] Mirkin, A. C., Chai, J., Huo, F., Zheng, Z,, Giam, R. L., "Block copolymer-assisted nanolithography," European Patent EP 2507668.

[6] Zhao et al., "SAXS Analysis of the Order−Disorder Transition and the Interaction Parameter of Polystyrene-block-poly(methyl methacrylate)," *Macromolecules* 41 (24), 9948–9951, 2008.

[7] Yokoyama et al.,"Self-Diffusion of Asymmetric Diblock Copolymers with a Spherical Domain Structure," *Macromolecules*, 31 (22), 7871–7876, 1998.

[8] Hardy et al., "Model ABC Triblock Copolymers and Blends Near the Order-Disorder Transition," *Macromolecules*, 35 (8), pp 3189–3197, 2002.

[9] Maeda et al. "Dual Mode Patterning of Fluorine-Containing Block Copolymers through Combined Top-down and Bottom-up Lithography," *Chemistry of Materials*, 24 (8), 1454–1461, 2012.

[10] Bates et al., "Polarity-Switching Top Coats Enable Orientation of Sub–10-nm Block Copolymer Domains," *Science* 338 (6108), 775-779, 2012.

[11] Jung et al. "A Path to Ultranarrow Patterns Using Self-Assembled Lithography," *Nano Letters,* 10 (3), 1000–1005, 2010.